Incorporation of Multi-Member Substructure Capabilities in FAST for Analysis of Offshore Wind Turbines

Preprint

H. Song, A. Robertson, and J. Jonkman
National Renewable Energy Laboratory

D. Sewell
University of Delaware

Presented at the Offshore Technology Conference
Houston, Texas
April 30–May 3, 2012

NREL is a national laboratory of the U.S. Department of Energy, Office of Energy Efficiency & Renewable Energy, operated by the Alliance for Sustainable Energy, LLC.

Conference Paper
NREL/CP-5000-53676
May 2012

Contract No. DE-AC36-08GO28308

Available electronically at http://www.osti.gov/bridge

Available for a processing fee to U.S. Department of Energy
and its contractors, in paper, from:

U.S. Department of Energy
Office of Scientific and Technical Information
P.O. Box 62
Oak Ridge, TN 37831-0062
phone: 865.576.8401
fax: 865.576.5728
email: mailto:reports@adonis.osti.gov

Available for sale to the public, in paper, from:

U.S. Department of Commerce
National Technical Information Service
5285 Port Royal Road
Springfield, VA 22161
phone: 800.553.6847
fax: 703.605.6900
email: orders@ntis.fedworld.gov
online ordering: http://www.ntis.gov/help/ordermethods.aspx

Cover Photos: (left to right) PIX 16416, PIX 17423, PIX 16560, PIX 17613, PIX 17436, PIX 17721

Printed on paper containing at least 50% wastepaper, including 10% post consumer waste.

OTC 23675

Incorporation of Multi-Member Substructure Capabilities in FAST for Analysis of Offshore Wind Turbines

Huimin Song, Amy Robertson, Jason Jonkman, National Renewable Energy Laboratory, and
DeAnna Sewell, University of Delaware

Abstract

The Fatigue, Aerodynamics, Structures, and Turbulence (FAST) code, developed by the National Renewable Energy Laboratory (NREL), is an aero-hydro-servo-elastic tool widely used for analyzing onshore and offshore wind turbines. This paper discusses recent modifications made to FAST to enable the examination of offshore wind turbines with fixed-bottom, multi-member support structures (which are commonly used in transitional-depth waters).

This paper addresses the methods used for incorporating the hydrostatic and hydrodynamic loading on multimember structures in FAST through its hydronamic loading module, HydroDyn. Modeling of the hydrodynamic loads was accomplished through the incorporation of Morison and buoyancy loads on the support structures. Issues addressed include how to model loads at the joints of intersecting members and on tapered and tilted members of the support structure.

Three example structures are modeled to test and verify the solutions generated by the modifications to HydroDyn, including a monopile, tripod, and jacket structure. Verification is achieved through comparison of the results to a computational fluid dynamics (CFD)-derived solution using the commercial software tool STAR-CCM+.

Introduction

Interest is growing in offshore wind turbines. Many offshore-wind-turbine support structures are being developed by modifying onshore wind turbine foundations, or oil and gas (O&G) industry structures. The offshore wind turbine support structures can be classified in three categories according to the water depth, as shown in Figure 1. In shallow water, where the water depth is less than 30 meters, monopiles and gravity bases that extend to the sea floor are used. In transitional depth, where the water depth is between 30 and 60 meters, new technologies are being created or adapted from the O&G industry, including jacket and multi-pile structures, which also extend to the sea floor. When the water depth is greater than 60 meters, a rigid structure fixed to the sea floor is no longer economical, and floating platforms may be required. This paper is focused on analyzing the support structures in transitional water depths.

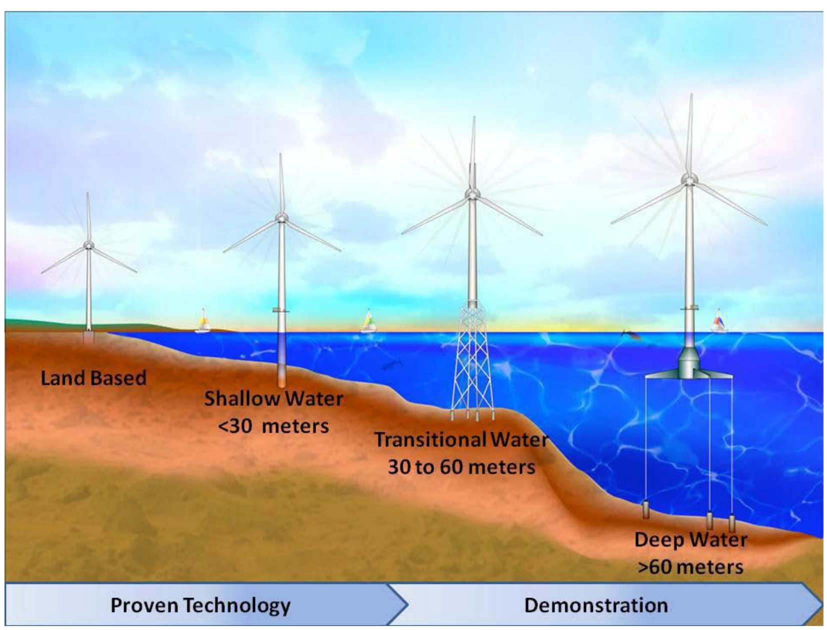

Figure 1: Status of offshore wind energy technology

Many design tools have been developed to analyze offshore support structures. FAST [1] is one such tool. FAST is an aero-hydro-servo-elastic tool developed by NREL for analyzing onshore and offshore wind turbines. Until now, FAST only had the capability of examining floating wind turbines and wind turbines with monopile support structures offshore (as well as land-based turbines). This paper examines recent modifications to FAST to enable the examination of offshore wind turbines with fixed-bottom, multi-member support structures, such as tripods and jackets.

The modifications include two steps. The first step is to model the hydrostatic and hydrodynamic loading on the structure through updates to FAST's HydroDyn module, and the second step is to model the structural dynamics of the support structure. This paper is focused only on the hydro-loading problem; the structural dynamics modeling work is ongoing. For the hydro-loading problem, the main components of analyzing offshore multi-member support structures in HydroDyn consist of correctly modeling the hydrostatic and hydrodynamic loading imparted to the structures by the water, including waves and currents.

In this paper, wave loads on three support structures—including a monopile, tripod, and jacket—are modeled using HydroDyn. The monopile and tripod models are created according to those outlined in the International Energy Agency (IEA) Wind Task 23 Subtask 2 Offshore Code Comparison Collaboration (OC3) project, and the jacket model is created according to the Task 30 OC3 Continuation (OC4) project. Load cases including still-water and linear regular waves are used to analyze the tripod and jacket models. The results are verified by comparing to results from CFD-based solutions using the commercial software tool STAR-CCM+.

HydroDyn Module

HydroDyn is the module within FAST that calculates hydrostatic and hydrodynamic loads on support structures for wind turbines. New functionality has been recently incorporated in HydroDyn to model loads on fixed-bottom, multi-member structures. Hydrodynamic loading for fixed-bottom, multi-member structures is modeled in HydroDyn using Morison and buoyancy loads with a strip theory approach. Effects caused by marine growth and flooded members are considered in the module as well. The previous version of HydroDyn also was capable of modeling Morison and buoyancy loads, but only for monopile or floating support structures.

Different from monopile support structures, multi-member support structures consist of not only vertical, uniform members, but also tilted, tapered, and connecting members, which make the analysis more complicated than before. When calculating buoyancy and hydrodynamic loads for multi-member support structures, there are a number of issues created by the overlapping of members at joints. Significant volumes are duplicated at the joints, as shown in Figure 2, distorting the overall level of wave and buoyancy loading, if not properly modeled. According to the OC3 project Phase III results [2], the overlapping volume is approximately 8% of the total volume below sea level for the tripod structure. Therefore, it has a significant effect on the buoyancy calculation as well as the applied Morison's equation forces.

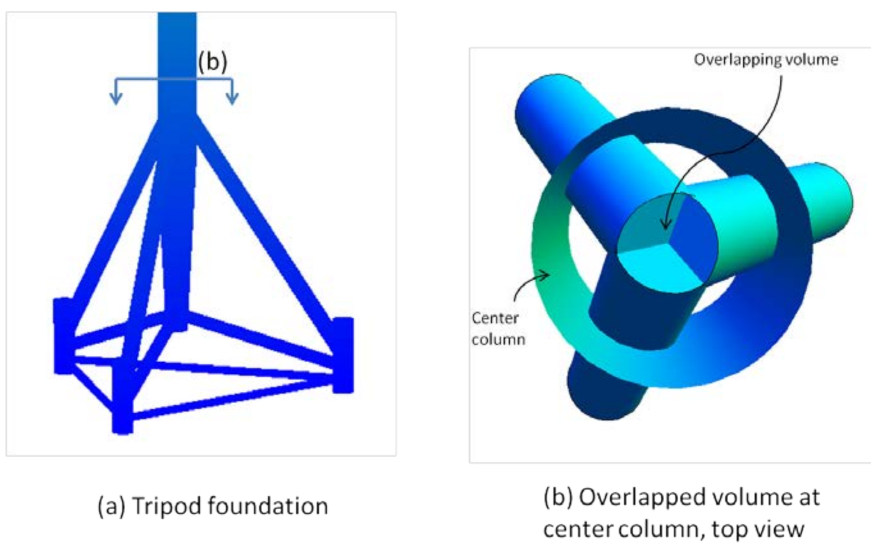

Figure 2: Tripod support structure

The flow chart of the HydroDyn code used to calculate hydrostatic and hydrodynamic loads on multi-member structures is shown in Figure 3. During initialization, HydroDyn reads an input file; reconstructs members and sets up markers; and calculates static buoyancy forces, marine growth, flooded forces and added mass. At each time step, HydroDyn will calculate the time-varying fluid-inertia forces, viscous drag forces, and dynamic-pressure forces at each marker.

To resolve the issue of overlapping at the joints, during initialization, HydroDyn reconstructs the multi-member support structures into a series of regular members and super members. Regular members are straight, uniform, or tapered cylinders.

A super member is used to represent some of the more complicated joints, and includes the overlapping parts of the members at the joint. Markers, which are nodes with a body-fixed coordinate system attached to them, are created at super members and intervals along the regular members. The hydrostatic and hydrodynamic loads are calculated at those markers.

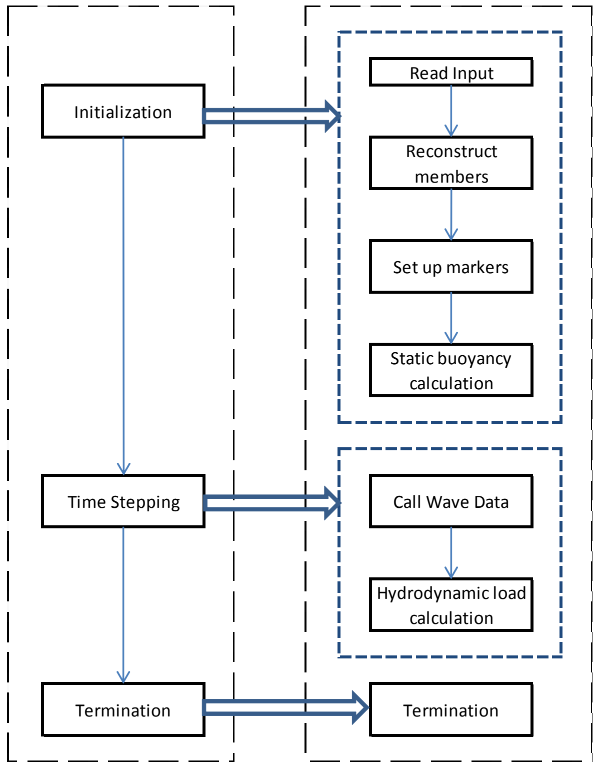

Figure 3: HydroDyn Flow Chart

Member reconstruction – super members

To take into account the overlap at the joints, an option is provided to construct a super member at the joint, so that the exact volume of the overlapping region is calculated. This option is only available if the members at the joint satisfy the following conditions: there are at least three members at the joint: at least two members are aligned at 180°: and the two 180° aligned members have the same diameter, which is greater or equal to the diameter of the adjoining members. The idea of the super member is to bound the intersecting region at the joint using boundary planes. For example, Figure 4 shows three members at one joint in two dimensions. Members 1 and 2 are aligned at 180°, and have the same diameter. These members are labeled as the master and second master members, respectively. Member 3 intersects with both members 1 and 2, and is labeled the slave member. The intersecting region is bounded by the planes AA', AA", BB' and the cylinder circumferences. This bounded region is labeled as a super member.

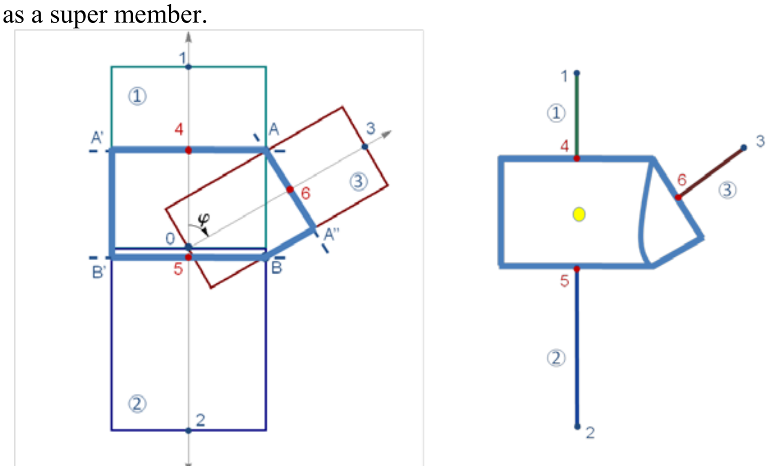

(a) Members at a joint before reconstruction

(b) Super member and updated regular members at the joint

Figure 4: Super member example

The volume of the super member can be obtained as:

$$V = \pi R_m^2 L_m + \sum_i \left(\pi R_{s_i}^2 L_{s_i} - V_c^i \right) \tag{1.1}$$

where R_m is the radius of master cylinders and L_m is the combined length of the master cylinders within the bounded region, i.e., the distance between points 4 and 5 in Figure 4(a). R_{s_i} is the radius of the i^{th} slave cylinder, L_{s_i} is the length from the joint to the corresponding boundary plane, i.e., the distance between points 0 and 6 in Figure 4(a). V_c^i is the common volume between the masters and the i^{th} slave cylinder. V_c^i can be calculated as follows:

$$\begin{aligned} V_c^i &= \frac{4}{3} R_m \csc\varphi_i \left[\left(R_m^2 + R_{s_i}^2 \right) \mathrm{EllipticE}\left(\frac{R_{s_i}^2}{R_m^2} \right) - \left(R_m^2 - R_{s_i}^2 \right) \mathrm{EllipticK}\left(\frac{R_{s_i}^2}{R_m^2} \right) \right],\ R_m > R_{s_i} \\ V_c^i &= \frac{8}{3} R^3 \csc\varphi_i,\ R_m = R_{s_i} = R \end{aligned} \tag{1.2}$$

where φ_i is the intersecting angle between the i^{th} slave and the master member, and $\mathrm{EllipticK}$ and $\mathrm{EllipticE}$ are the complete elliptic integrals of the first and the second kind respectively.

Markers

After reconstructing members, all members can be divided into two types. One type is the regular member, which is a straight cylinder, either uniform or tapered. The other type is the super member, which is a combination of intersecting cylinders.

The regular members have markers placed along their lengths according to the division size defined by the user. In Figure 5, the blue markers are interior markers. If the member is not connected to a super member, then an end marker is set at the end of the member, which is shown as orange dots in the figure. If the member is connected to a super member, then we set no marker at the connecting end of this member. Each marker will have information such as the position, the direction cosines between local and global coordinate systems, the diameter, and the tapered ratio, etc.

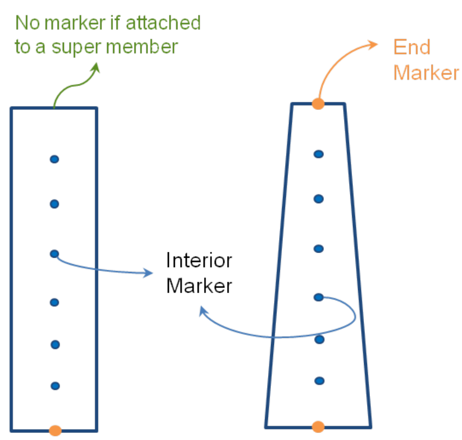

Figure 5: Regular member markers

The super member marker is set at the center of the combined master member. Concentrated forces are calculated at the super member marker. The super member marker has information such as position, master direction cosine matrix, slave members direction cosines, end cap positions, and radii of all submembers.

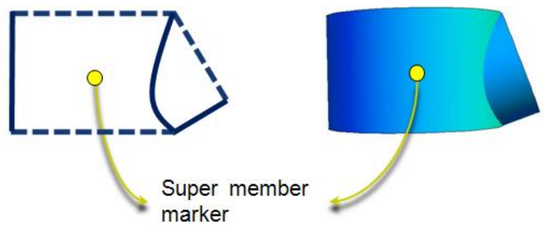

Figure 6: Super member marker

Load calculation

At each marker, loads are calculated according to the marker type and position. There is no calculation if the marker position is below the mud line or above the still-water level (SWL); or, if wave stretching is applied, above the instantaneous free surface (IFS). For interior markers, distributed hydrostatic and hydrodynamic forces and moments (per unit length) are calculated. For end markers and super member markers, concentrated hydrostatic and hydrodynamic forces and moments are calculated. While not explicitly defined here, hydrodynamic added mass caused by structural acceleration is also calculated.

Hydrostatic load calculation

The static buoyancy force is calculated by integrating the static water pressure distribution over the wetted surface area of the cylinder. (If the member is flooded, both outer and inner surface area will be used.) Through analytical derivation, these integrations lead to the formulation described below, which is how they are implemented in HydroDyn. If the marker is positioned between the SWL and the mudline, we assume the cross-section at the marker is fully submerged.

Interior marker

For an interior marker, the distributed buoyancy forces and moments are calculated at the marker as:

$$\boldsymbol{F}_B = \rho g \begin{bmatrix} C_{31}\pi R^2 & C_{32}\pi R^2 & -2\pi R\frac{\partial R}{\partial z}Z & C_{32}\frac{\partial R}{\partial z}\pi R^3 & -C_{31}\frac{\partial R}{\partial z}\pi R^3 & 0 \end{bmatrix}^T \tag{1.3}$$

where $\boldsymbol{F}_B$ is a load per unit length, and is expressed in the member local coordinate system; the first three terms represent forces per unit length and the second three terms represent moments per unit length. ρ and g are the fluid density and gravitational acceleration constant, respectively. z is the coordinate in the member local coordinate system, Z is the coordinate in the global coordinate system, R is the radius at the marker, and C_{ij} are the components of the member direction cosine matrix, which is non-zero for tilted members. $\frac{\partial R}{\partial z}$ is the tapered ratio in the member local coordinate system and is non-zero only for tapered members.

End marker

For the end marker, concentrated buoyancy forces and moments in the local coordinate system are calculated at the marker as:

$$\boldsymbol{F}_B = \rho g \begin{bmatrix} 0 & 0 & -Z\pi R^2 & \frac{\pi}{4}C_{32}R^4 & -\frac{\pi}{4}C_{31}R^4 & 0 \end{bmatrix}^T \tag{1.4}$$

If the end marker has an outward normal opposite of the member direction, the buoyancy forces in the equation above have opposite signs.

Super member marker

For the super member marker, concentrated buoyancy forces in the global coordinate system are calculated by using the displaced super member volume (V) times ρg and subtracting the contribution from the end cap surfaces as follows:

$$\boldsymbol{F}_B = \begin{bmatrix} 0 & 0 & \rho g V & 0 & 0 & 0 \end{bmatrix}^T - \sum \boldsymbol{F}^i_{\mathrm{glb}} \tag{1.5}$$

where $\boldsymbol{F}^i_{\mathrm{glb}}$ is the point buoyancy forces at the end cap of the i^{th} member, and can be calculated using the end point equation in (1.4) (with moments set to zeros) and then transformed to the global coordinate system. $\boldsymbol{F}_B$ is expressed in the global coordinate system. The moment at the super member is set to zero, because a test calculation showed that the moment at the supermember is small compared to other loads.

Hydrodynamic load calculation

At each marker, the hydrodynamic load $\boldsymbol{F}$ is calculated as $\boldsymbol{F} = \boldsymbol{F}_I + \boldsymbol{F}_D + \boldsymbol{F}_{DP}$, where $\boldsymbol{F}_I$ is the inertia force, $\boldsymbol{F}_D$ is the drag force, and $\boldsymbol{F}_{DP}$ is the dynamic pressure force. The inertia and drag forces are calculated using terms from Morison's equation. The dynamic pressure force is calculated by integrating the dynamic pressure over the wetted surface area (evaluated with the formulation given below). The hydrodynamic moments are assumed to be negligible.

Interior marker

At interior markers, distributed forces (per unit length) are calculated as:

$$
\begin{aligned}
\boldsymbol{F}_I &= \left(C_A + 1\right)\rho\pi R^2 \left(\vec{k} \times \vec{a}_f \times \vec{k}\right) \\
\boldsymbol{F}_D &= C_D \rho R \left|\vec{k} \times \vec{v}_{rel} \times \vec{k}\right| \left(\vec{k} \times \vec{v}_{rel} \times \vec{k}\right) \\
\boldsymbol{F}_{DP} &= \begin{bmatrix} 0 & 0 & 2\pi R \dfrac{\partial R}{\partial z} p_{dyn} \end{bmatrix}^T
\end{aligned}
\tag{1.6}
$$

where $\boldsymbol{F}_I$ and $\boldsymbol{F}_D$ are terms from Morison's equation expressed in the global coordinate system and $\boldsymbol{F}_{DP}$ is expressed in the member local coordinate system. C_A is the added mass coefficient and C_D is the viscous drag coefficient. $\vec{k} = C_{13}\vec{I} + C_{23}\vec{J} + C_{33}\vec{K}$ is the cylinder member axial unit vector in the global coordinate system at the marker. $\vec{a}_f$ is the fluid acceleration vector at the marker. $\vec{v}_{rel}$ are the relative velocity vectors at the marker, where $\vec{v}_{rel} = \vec{v}_f - \vec{v}_s$, $\vec{v}_f$ and $\vec{v}_s$ are the fluid and structure velocity vectors at the marker. p_{dyn} is the dynamic pressure at the marker. The wave and current kinematics are calculated in the absence of the structure; details are given in [3].

End marker

End markers are modeled as thin circular sheets; therefore, the inertia force is not considered. At end markers, concentrated forces are calculated as:

$$
\begin{aligned}
\boldsymbol{F}_I &= 0 \\
\boldsymbol{F}_D &= \frac{1}{2} C_D \rho\pi R^2 \left|\vec{k} \times \vec{v}_{rel} \times \vec{k}\right| \left(\vec{k} \times \vec{v}_{rel} \times \vec{k}\right) \\
\boldsymbol{F}_{DP} &= \begin{bmatrix} 0 & 0 & \pi R^2 p_{dyn} \end{bmatrix}^T
\end{aligned}
\tag{1.7}
$$

Super member marker

At super member markers, concentrated forces are calculated as:

$$
\begin{aligned}
\boldsymbol{F}_I &= \left(C_A + 1\right)\rho V \left(\vec{k}_m \times \vec{a}_f \times \vec{k}_m\right) \\
\boldsymbol{F}_D &= \frac{1}{2} C_D \rho A \left|\vec{k}_m \times \vec{v}_{rel} \times \vec{k}_m\right| \left(\vec{k}_m \times \vec{v}_{rel} \times \vec{k}_m\right) \\
\boldsymbol{F}_{DP} &= 0
\end{aligned}
\tag{1.8}
$$

where V is the actual volume of the super member, $\vec{k}_m$ is the unit direction vector of the master cylinder member axis. The dynamic pressure force is approximated to be zero to simplify the calculation. The area A is an equivalent projection area perpendicular to the wave direction. A can be approximated from the total super member volume V and the length of the combined master member within the bounded region L_m as:

$$
A = 2\sqrt{\frac{VL_m}{\pi}} \tag{1.9}
$$

Marine growth and flooded members

Marine growth is taken into account by increasing the outer diameter of the structural member in the calculation of the hydrostatic and hydrodynamic wave loads and by adding weight to the structure. Modeling of flooded members is included through calculation of hydrostatic forces and moments caused by flooded sea water at each marker; these calculations are solved using the same equations as used by the buoyancy force calculation, but with opposite sign and the inner radius applied.

Results

Three support-structure types are examined in this paper to assess the accuracy of the implemented theory, including a monopile, a tripod, and a jacket (see Figure 7). All three structures were modeled in HydroDyn, and also in the CFD-code, STAR-CCM+, for comparison purposes. Two load cases were run, a still-water case and a linear regular wave condition case. For all simulations, the structures are considered to be rigid, the density of the sea-water is set to 1,025 kg/m^3, and wind is not considered.

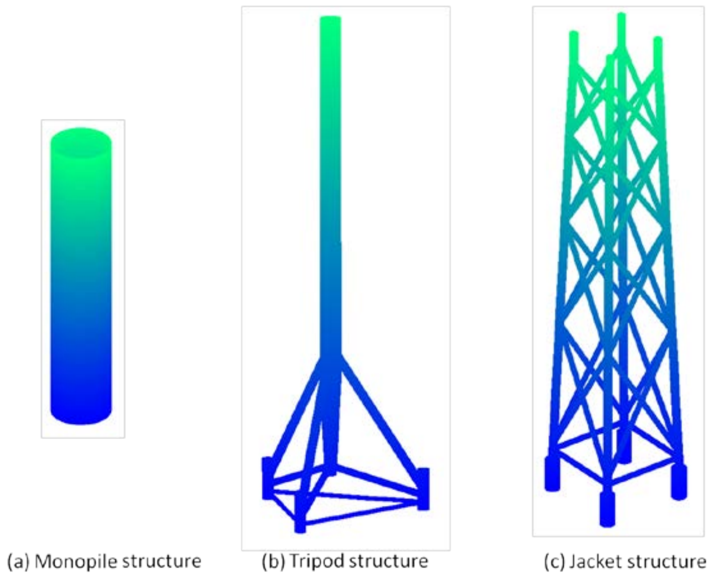

Figure 7: Tripod and jacket structure

Models

Three example structures are modeled to test and verify the solutions generated by the modifications to HydroDyn, including a monopile, tripod, and jacket structure. The publicly available structures used in the IEA OC3 and OC4 projects were applied here. These structures were chosen to span the design space for support structures of bottom-fixed offshore wind turbines.

The monopile foundation (see Figure 7(a)) is a rigid structure cantilevered at the mudline, with a constant diameter of 6 m and a constant thickness of 0.060 m. The monopile extends from the tower base, which is at an elevation of 10 m above the mean-sea level, to the mudline, which is at 20 m below SWL [2].

The tripod is modeled as a rigid structure cantilevered at the mudline at a 45-m water depth. The tripod is one of the space-frame concepts proposed for offshore installations in water of intermediate depth. The tripod support structure is shown in Figure 7(b); the details can be found in [4]. The tripod structure presents several features that are not included in the traditional monopile structure, such as an asymmetric structure, inclined members, multiple members connected at one joint, and a significantly tapered center column.

The jacket foundation was originally designed by RAMBØLL A/S [5] for the UpWind Project. The design was adopted for the OC4 project at a water depth of 50 m, as shown in Figure 7(c). The structure is cantilevered at the mud line. Compared to the tripod, the jacket foundation has some new features such as allowances for marine growth and flooded members. In this paper, the marine growth and flooded members are not modeled in the simulation.

The simulations performed in STAR-CCM+ model the flow field using the Reynolds-Averaged Navier-Stokes equations. Turbulence is modeled with the k-omega eddy viscosity model with a two-layer all y+ wall treatment. Each structure is placed into the middle of the computational domain that extends 400 m long, 200 m wide, and 150 m high. The structures are represented by a wall that is rigidly mounted to the domain bottom, representing the sea floor as a wall. A no-slip condition on the velocity is imposed on the wall boundaries. Flow enters the domain at the left-end boundary at a flow-inlet, moving from left to right, and exits the domain at a pressure outlet. A wave damping condition is enforced 100 m upstream of the outlet, providing a vertical resistance to motion to dampen outgoing waves and to prevent wave reflection. Symmetry planes represent the remaining boundaries. Each solution domain is decomposed into a finite number of cell-centered control volumes, yielding an overall mesh that is both unstructured, containing arbitrary shapes, and adaptive, with local refinement near the free surface and near structure boundaries. A maximum cell-volume-face size of 0.125 m was imposed on each structure to capture the complex member orientations. Additionally, prism-layer cells were put on the structure surface to resolve the viscous sub-layer using a y+ number of about 100. The governing equations were discretized over the described mesh, and solved using the transient SIMPLE algorithm solver. Time is advanced using a second-order implicit scheme.

Simulations

Still-water case

In the still-water case, the wave velocity and acceleration are zero. Therefore, only the static buoyancy is calculated.

Monopile model

There is no static buoyancy for the monopile model because the monopile is cantilevered at the mud line and it is not tapered. The HydroDyn calculation shows a value close to zero (in the scale of 10^{-9} N) for the forces at all markers, which agrees with the results from the STAR-CCM+ calculation.

Tripod model

The total buoyancy is calculated for the tripod structure. The results from HydroDyn are compared to the results from STAR-CCM+. The overall buoyancy for the whole structure is 7.33E6 N from the HydroDyn calculation, and 7.46E6 N from STAR-CCM+. The buoyancy value is positive, which means that it is providing an upward force to the structure. The difference in value between HydroDyn and STAR-CCM+ is small, and can be attributed to small differences in the way that the intersection of the members at the joints is being modeled—e.g., in HydroDyn, the tapering in the super member is not considered.

Jacket model

The total buoyancy is calculated on the jacket foundation structure. The results from HydroDyn are compared to the results using STAR-CCM+. The overall buoyancy for the whole structure is -2.127E6 N from the HydroDyn calculation, and -2.137E6 N from STAR-CCM+, which is very good agreement. Note that the buoyancy force is now negative, which means it is actually providing a downward force to the structure. The reason that the force is downward is because of the tapering of the legs, which get wider at the bottom. There is also a large pressure on the top surface of the piles because the piles have a larger diameter than the legs, which introduces a large negative buoyancy force in the vertical direction.

Linear regular wave

In this load case, a linear wave is applied to the three structures. For the monopile, the wave has a height of 0.6 m and a period of 10 s. For the tripod, a wave with a height of 1.0 m and a period of 10 s is used. Finally, for the jacket, a wave with a height of 1.4 m and a period of 10 s is used. The wave heights are chosen as high as possible while still ensuring that Airy linear wave theory is fully valid. For each case 30 s simulation results are compared for both methods. Wheeler stretching is applied to the wave kinematics in the HydroDyn results. Results from STAR-CCM+ are still pending for this load case for the jacket and tripod structures, so only the results from HydroDyn are shown for these structures. A comparison between STAR-CCM+ and HydroDyn are shown for the monopile model.

Monopile model

The overall hydrodynamic force on the monopile under regular wave loading is calculated using HydroDyn and STAR-CCM+, and the results are shown in Figure 8. As shown in this figure, the forces in the x-direction fluctuate about a mean value of zero because there is no buoyancy on the monopile structure. The periodicity of the solution aligns with the periodicity of the waves hitting the structure. The forces in the y and z directions are zero for both methods. From the figure shown here, one can observe that the results from HydroDyn and STAR-CCM+ have good agreement.

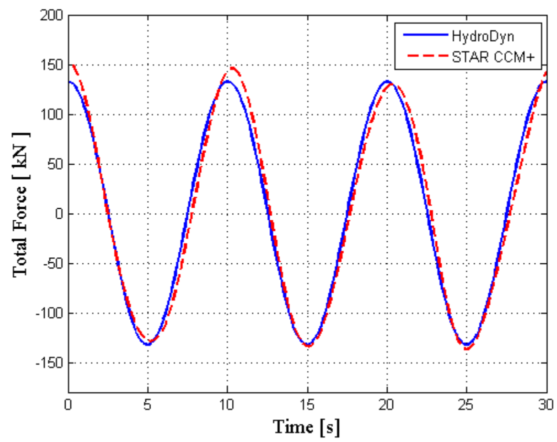

Figure 8: Total force in x-direction for monopile support structure

Figure 9 shows the distributed forces in the x-direction at three different water depths, which are $z = -0.125$ m, $z = -10.0$ m, and $z = -19.875$ m. From the figure, one can observe that close to the SWL, where $z = -0.125$ m, the surface wave has a significant effect on the wave loads on the structure, This location is periodically submerged because of the instantaneous wave elevation change, which can be observed from both methods, while STAR-CCM+ presumably captures the surface effect more accurately than HydroDyn. At deeper water depths, where $z = -10.0$ m, and $z = -19.875$ m, the results from both methods have very good agreement.

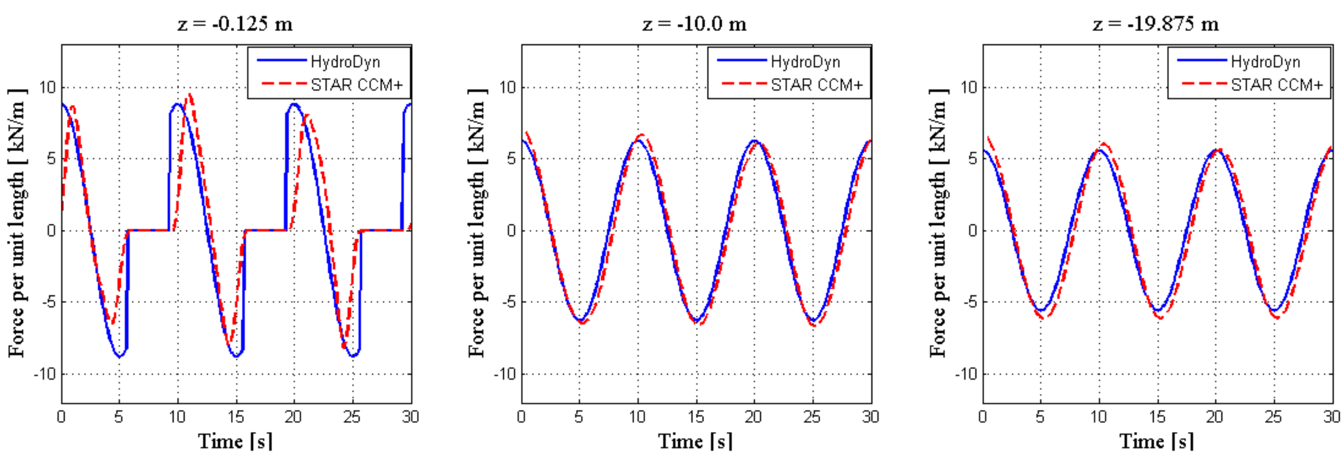

Figure 9: Distributed force in x-direction at different water depths for monopile model

Tripod mode

The overall hydrodynamic force on the tripod under regular wave loading is calculated using HydroDyn, and the results are shown in Figure 10. As shown in this figure, the forces in the x- and z-directions fluctuate; in the z-direction, the fluctuation is about a nonzero mean value, which is the static value presented previously. The forces in the y-direction are zero, because both the wave and the tripod structure are symmetric about the y axis. Without waves, the only force on the structure is in the z-direction. The periodicity of the solution aligns with the periodicity of the waves hitting the structure.

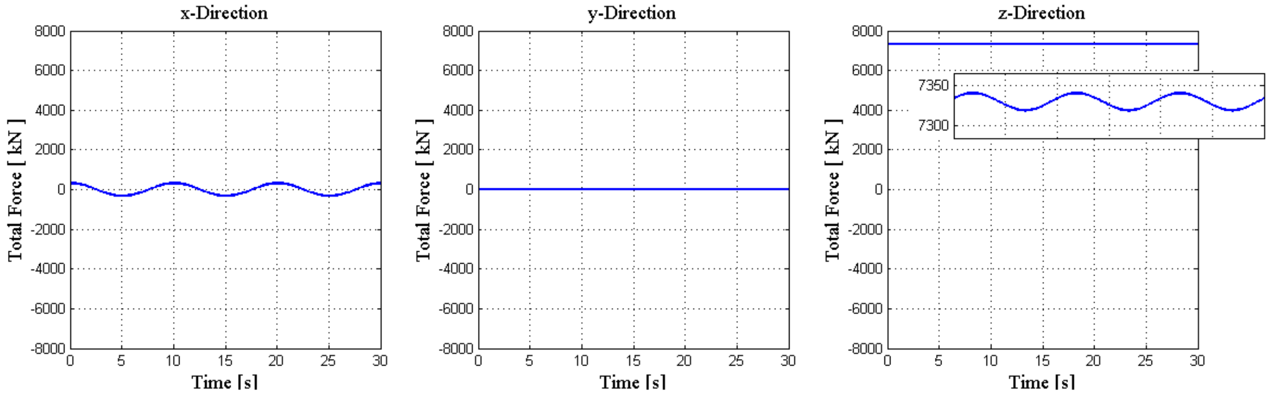

Figure 10: Tripod support structure

Jacket model
The overall hydrodynamic force on the jacket under regular wave loading is calculated using HydroDyn, and the results are shown in Figure 11. The results are similar to that shown for the tripod. The solution is periodic, based on the wave frequency, and oscillates about a mean static value in the z-direction. In this case, the mean value in the z-direction is negative, indicating a downward force on the structure from the water.

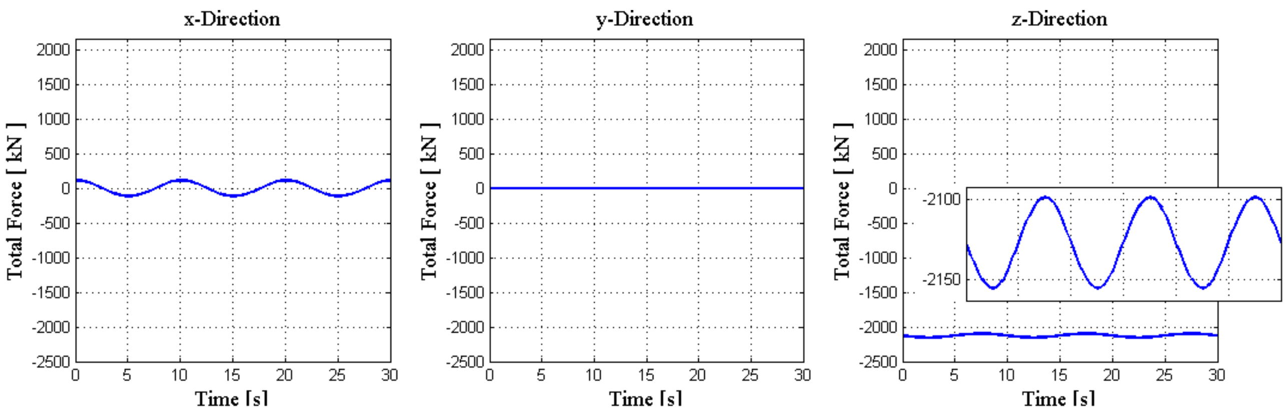

Figure 11: Jacket support structure

Conclusions

This paper summarizes recent work done at NREL to expand the capabilities of its in-house wind turbine simulation tool, FAST, to model fixed-bottom, multi-member offshore support structures. These types of structures are the industry standard designs for wind turbines placed in transitional depth waters (30-60 m), and include tripods and jackets. The present release-version of FAST includes the capability of analyzing land-based wind turbines, as well as the common designs for shallow and deep water, which are monopiles and floating platforms, respectively. Thus, this new work will allow FAST to model most fixed-bottom substructures, including industry-standard support-structure designs for wind turbines placed in all water depths.

This work so far has only focused on incorporating the hydrodynamic loading for multi-member structures. Future work will focus on the modeling of the structural dynamics of fixed-bottom support structures that are not monopiles.

To verify the accuracy of the hydrodynamic loading models incorporated into HydroDyn, the hydrodynamics module within FAST, simulation results were compared to a CFD-tool, STAR-CCM+. Three different support structure models were used to compare the results—a monopile, tripod, and jacket. This paper showed that the static buoyancy calculations from HydroDyn and STAR-CCM+ were very similar. Results of the hydrodynamic loading on these structures under forcing from waves were also shown from HydroDyn. Results from STAR-CCM+ for the tripod and jacket are still being computed, and could not be compared in this paper. The results for the monopile from HydroDyn and STAR-CCM+ show good agreement. The initial results for the tripod and jacket from HydroDyn look promising, showing a periodic variation of the hydrodynamic loading on the structure which follows the periodicity of the waves about the still-water load value.

Future work will focus on performing more comparisons between the results provided by HydroDyn and a CFD-based solution. Simulations will be run to examine the hydrodynamic loading on the structures under a variety of wave scenarios and the complex loading around the joints of the tripod and jacket will be assessed for further verification of the HydroDyn implementation. Once the structural dynamics capabilities for fixed-bottom, multi-member structures are incorporated into FAST, comparisons will also be made to the results from the OC3 and OC4 projects for the tripod and jacket structures, respectively.

References

[1] Jonkman, J.M.; Buhl Jr., M.L. *FAST User's Guide*. NREL/EL-500-29798. Golden, Colorado: National Renewable Energy Laboratory, 2005.

[2] Jonkman, J; Musial, W., "Offshore Code Comparison Collaboration (OC3) for IEA Task 23 Offshore Wind Technology and Deployment." Technical Report, NREL/TP-5000-48191, December 2010.

[3] Jonkman, J.M. *Dynamics Modeling and Loads Analysis of an Offshore Floating Wind Turbine*. Ph.D. Thesis. Department of Aerospace Engineering Sciences, University of Colorado, Boulder, CO, 2007; NREL/TP-500-41958. Golden, CO: National Renewable Energy Laboratory.

[4] Camp, T. OC3 internal communication from GH, tower definition_NEW.xls, March 11, 2008.

[5] Vemula, N. K.; DeVries, W.; Fischer, T.; Cordle, A.; Schmidt, B. (2010). "Design solution for the upwind reference offshore support structure." Upwind deliverable D4.2.6 (WP4: O_shore foundations and support structures), Ramb_ll Wind Energy.